

# POLARIZATION OF SYNCHROTRON EMISSION FROM RELATIVISTIC RECONFINEMENT SHOCKS

KRZYSZTOF NALEWAJKO & MAREK SIKORA

*Nicolaus Copernicus Astronomical Center, ul. Bartycka 18, 00-716 Warsaw, Poland*

We study the dynamical structure of relativistic reconfinement shocks and the characteristics of associated synchrotron emission to extend theoretical basis for interpreting polarimetric observations of AGN jets. Many properties of reconfinement shocks are governed by a single parameter, which is a product of jet Lorentz factor  $\Gamma_j$  and half-opening angle  $\Theta_j$ . Shocks with  $\Gamma_j\Theta_j > 1$  are very efficient energy dissipators. We calculate linear polarization produced from various magnetic field components: the chaotic one compressed at the shock surface, and the large-scale helice of various pitch angles. We have obtained a wide range of polarization states, depending on the relative strength of these components.

## ROLE OF RECONFINEMENT SHOCKS IN AGN JETS

Interaction of astrophysical jets with their environment can lead to formation of oblique stationary shocks. In AGN jets they are expected to collimate at the distance determined by the ratio of jet power  $L_j$  and external pressure  $p_e$  [1]:

$$z_r \sim 0.7 \sqrt{\frac{L_j}{p_0 c}} \sim 0.9 \sqrt{\frac{L_{j,46}}{p_{0,-2}}} \text{ pc}. \quad (1)$$

Reconfinement shocks have been linked to stationary knots, such as the peculiar HST-1 knot in M87 [2]. They have also been proposed as an energy dissipation mechanism responsible for the 2005 flare in 3C 454.3 [3].

We have developed a semi-analytical model for the structure of relativistic reconfinement shocks. Shock-jump equations are solved in hydrodynamical approximation, the effect of radiative losses is accounted for in post-shock equation of state. Synchrotron emissivity is taken to be a fraction of energy dissipation rate. Synchrotron polarization degree is calculated for electron power-law index  $p = 2$  ( $\Pi_{max} \sim 0.7$ ). We calculate Doppler factors and Stokes parameters for each shock surface portion and use them to produce emission maps.

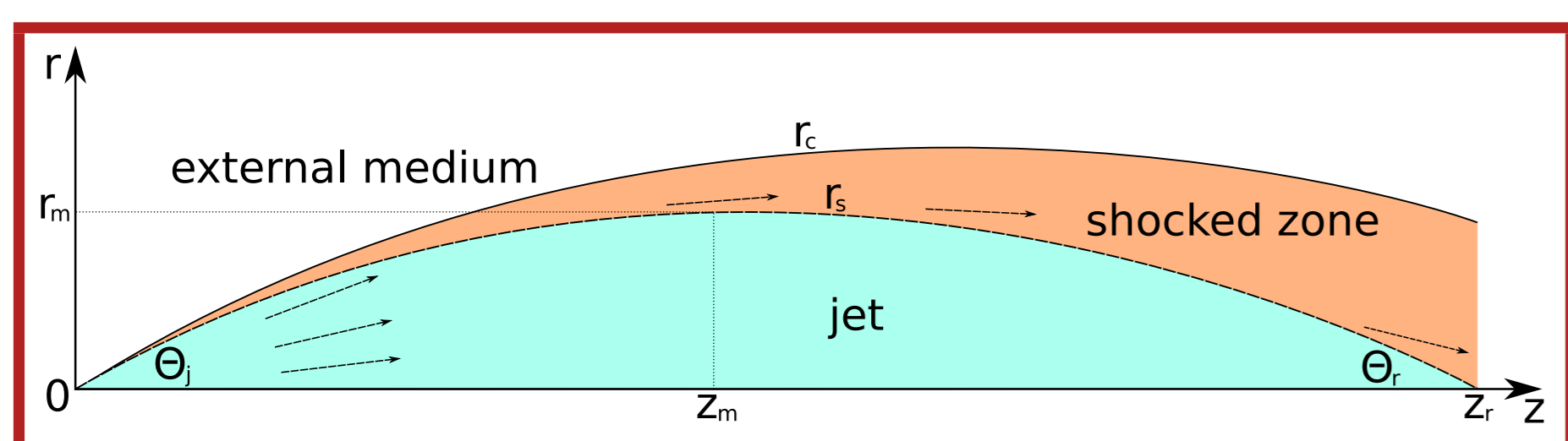


Figure 1: Model of reconfinement shocks.

## ENERGY DISSIPATION EFFICIENCY

We define energy dissipation efficiency as a relative change in kinetic energy flux across shock surface element. When averaged over the whole structure, it depends primarily on the product of jet Lorentz factor  $\Gamma_j$  and opening angle  $\Theta_j$ .

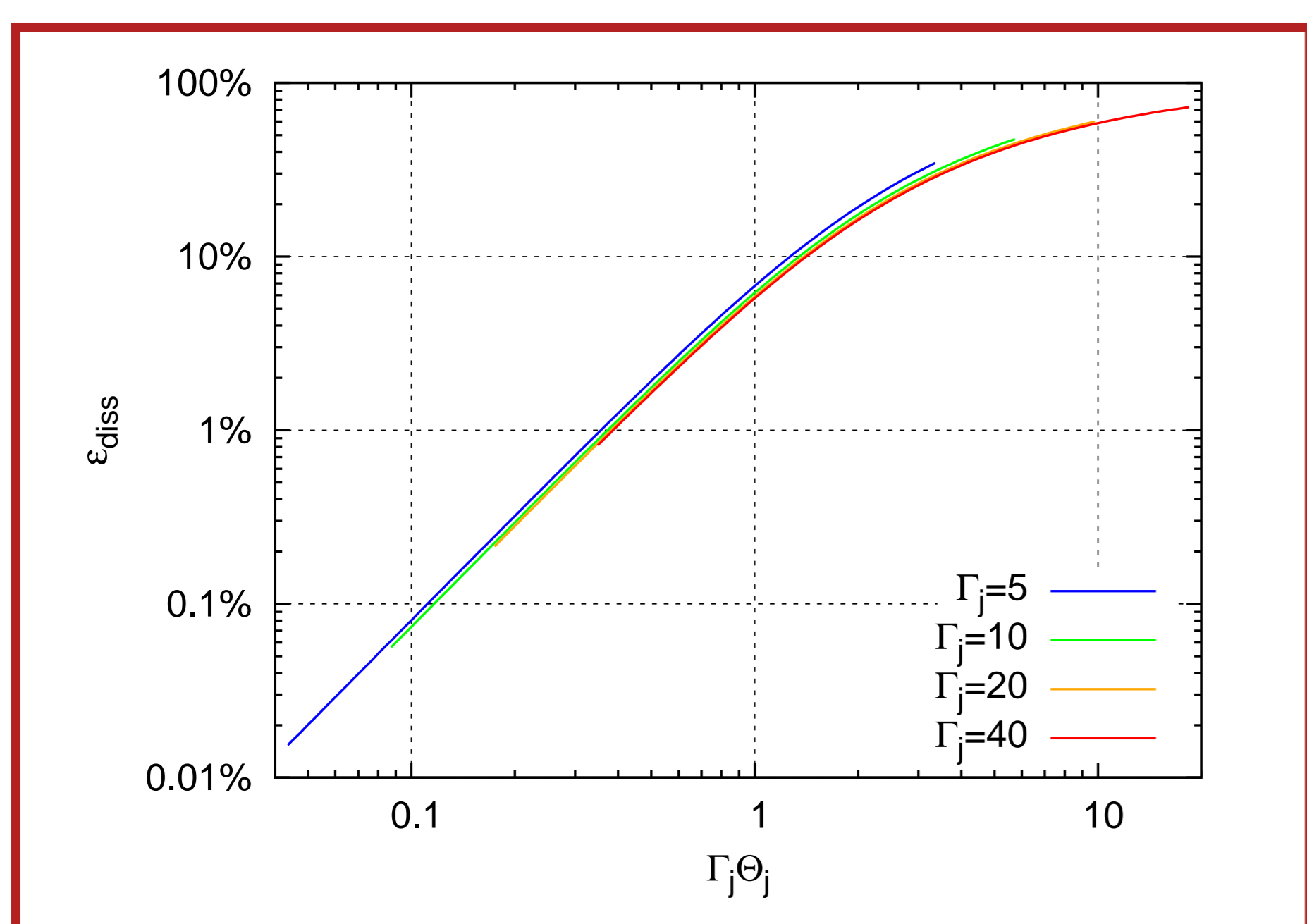


Figure 2: Energy dissipation efficiency  $\epsilon_{diss}$  as a function of  $\Gamma_j\Theta_j$ . Models calculated for different values of  $\Gamma_j$  yield very similar results.

We have found that the efficiency can be high for  $\Gamma_j\Theta_j > 1$ , while for  $\Gamma_j\Theta_j < 1$  we provide an estimate  $\epsilon_{diss} \sim 6\%(\Gamma_j\Theta_j)^2$  [4]. This can be considered as an upper limit, as for jets carrying significant internal and/or magnetic energy it would be much lower.

A knowledge of  $\Theta_j$  is required to assess potential dissipation efficiency. A good proxy of it is the reconfinement shock aspect ratio  $r_m/z_r \sim \Theta_j/4$ .

High dissipation efficiency via reconfinement shocks is plausible in AGN jets, but even more so during the initial phase of long GRBs [5].

## POLARIZATION FROM CHAOTIC MAGNETIC FIELDS

Polarization from shock-compressed chaotic MFs has been calculated for the case of relativistic conical shocks [6]. They have found, that even highly oblique shocks produce parallel polarization ( $Q > 0$ , corresponding to perpendicular MFs), while the degree of perpendicular polarization ( $Q < 0$ ) is limited by 10%.

We have found quite an opposite situation for reconfinement shocks: they are dominated by perpendicular polarization with degrees up to 30%, but can produce some parallel polarization, if  $\Gamma_j\Theta_j > 1$  and  $\theta_{obs} < \Theta_j$  [7].

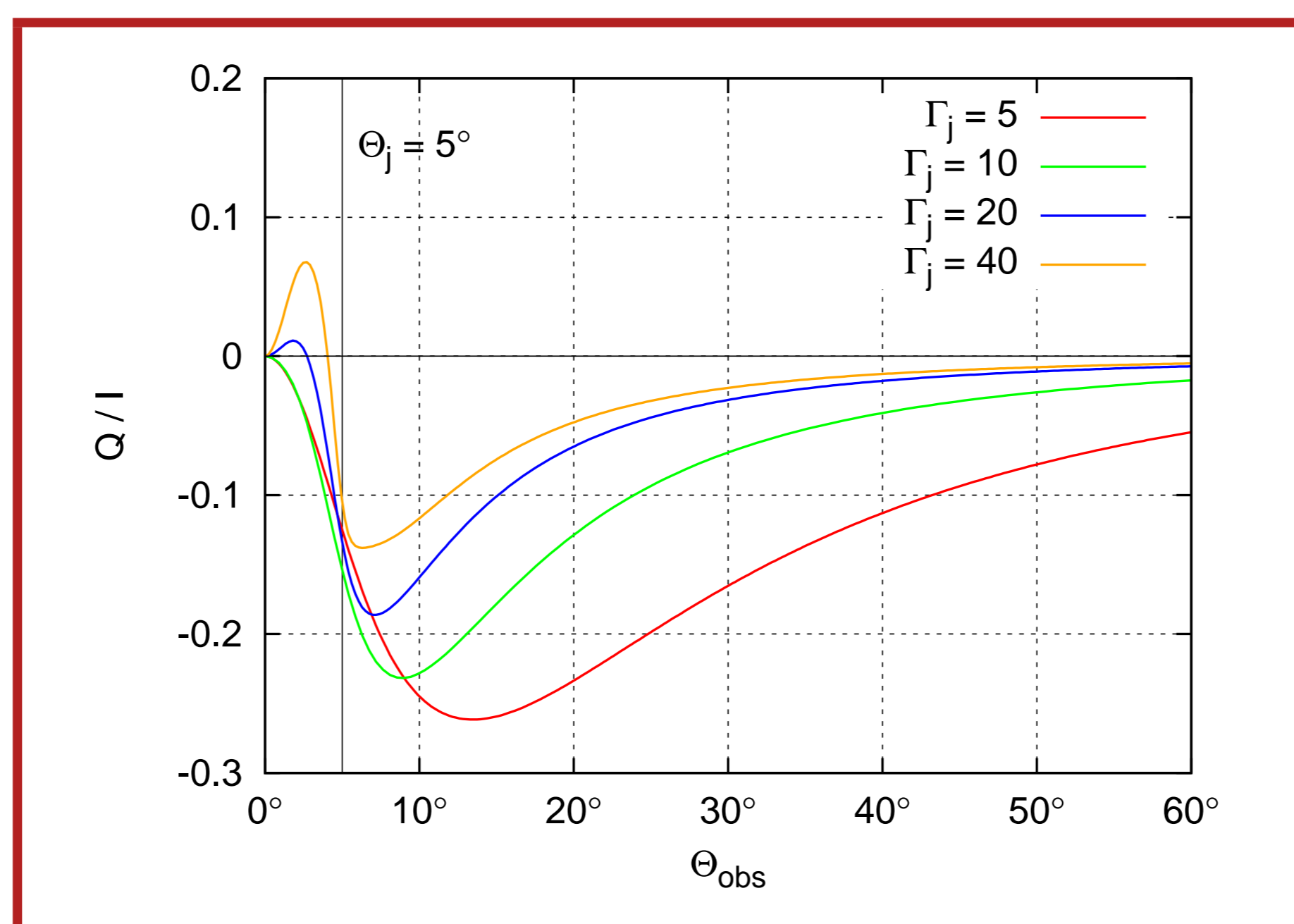


Figure 3: Spatially averaged polarization as a function of the observer position angle  $\theta_{obs}$  relative to the jet axis. The models are calculated for half-opening angle  $\Theta_j = 5^\circ$ , and for a range of jet Lorentz factors  $\Gamma_j$ . Note that  $1/\Theta_j \approx 11.5$ , thus we cover here both  $\Gamma_j\Theta_j < 1$  and  $\Gamma_j\Theta_j > 1$  regimes.

We have also produced synthetic polarization maps, as would be measured from different positions. We note, that Doppler boosting strongly modifies total intensity maps for  $\theta_{obs} \leq \Theta_j$ , a second brightness peak would appear close to the projected shock origin. In this case the brightness peaks produce parallel polarization that can balance perpendicular polarization from other shock portions.

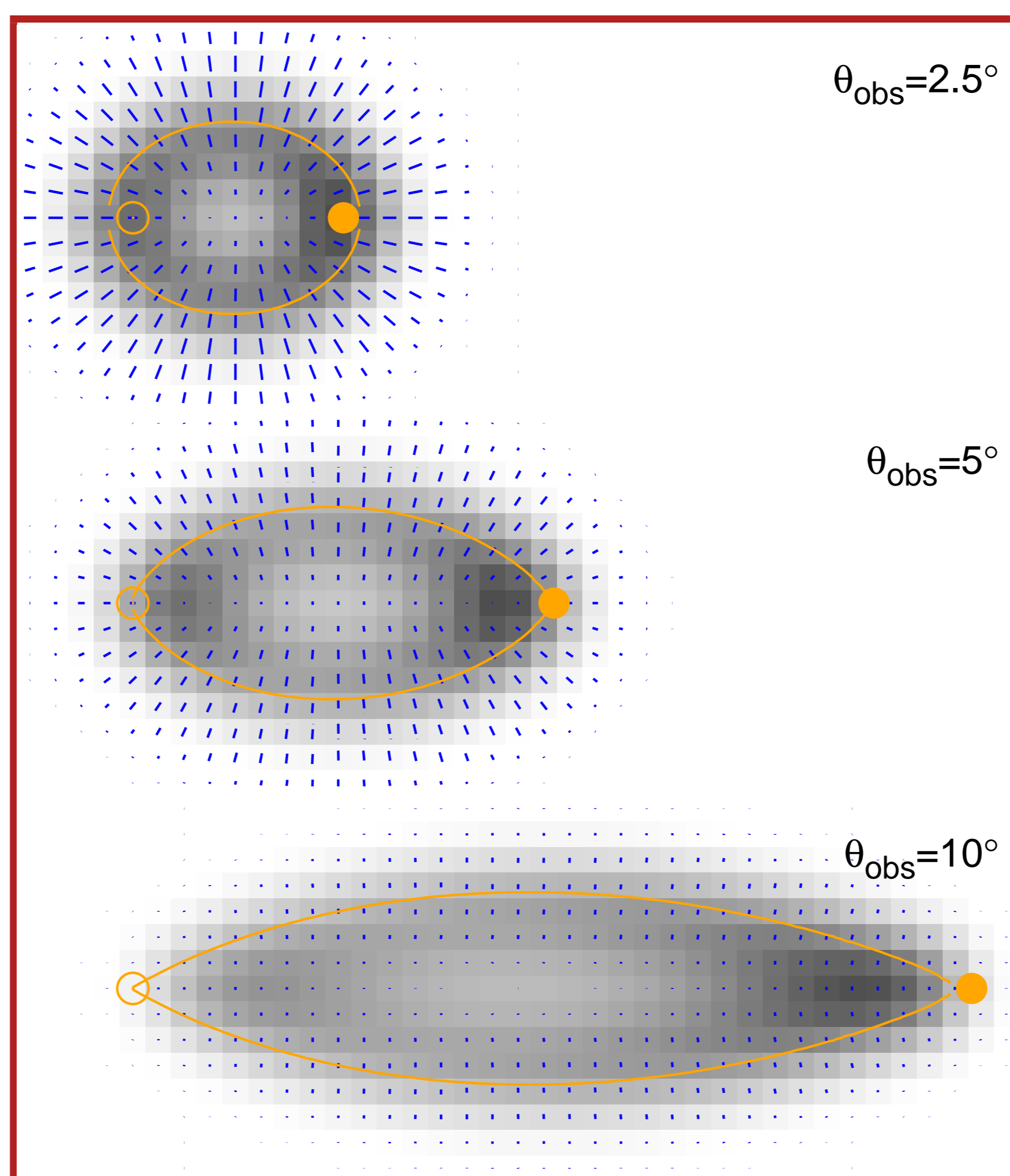


Figure 4: Polarization maps resulting from jet model with  $\Gamma_j = 10$  and  $\Theta_j = 5^\circ$  for three different observers with given  $\theta_{obs}$ . Jet origin is marked with empty circle, recollimation point with filled circle. Gray shading shows total brightness distribution, while blue bars mark polarization electric vectors.

## POLARIZATION FROM ORDERED MAGNETIC FIELDS (PRELIMINARY)

We can add a large-scale helical MF component of varying strength and pitch angle. The structure of this component is governed by magnetic energy flux conservation laws in unshocked zone, as well as shock-jump conditions for magnetic fields frozen into plasma. We choose an arbitrary transverse scaling law for toroidal MF component – that it is proportional to the radial coordinate.

The purely toroidal MF produces high parallel polarization. Averaged polarization from reconfinement shocks is very sensitive to the amount of toroidal MF added to chaotic MF. Introducing non-vanishing poloidal MF component (non-zero helical MF pitch angle  $\alpha_B$ ), we obtain dominance of perpendicular polarization for  $\alpha_B > 5^\circ$  (as measured at jet maximum width).

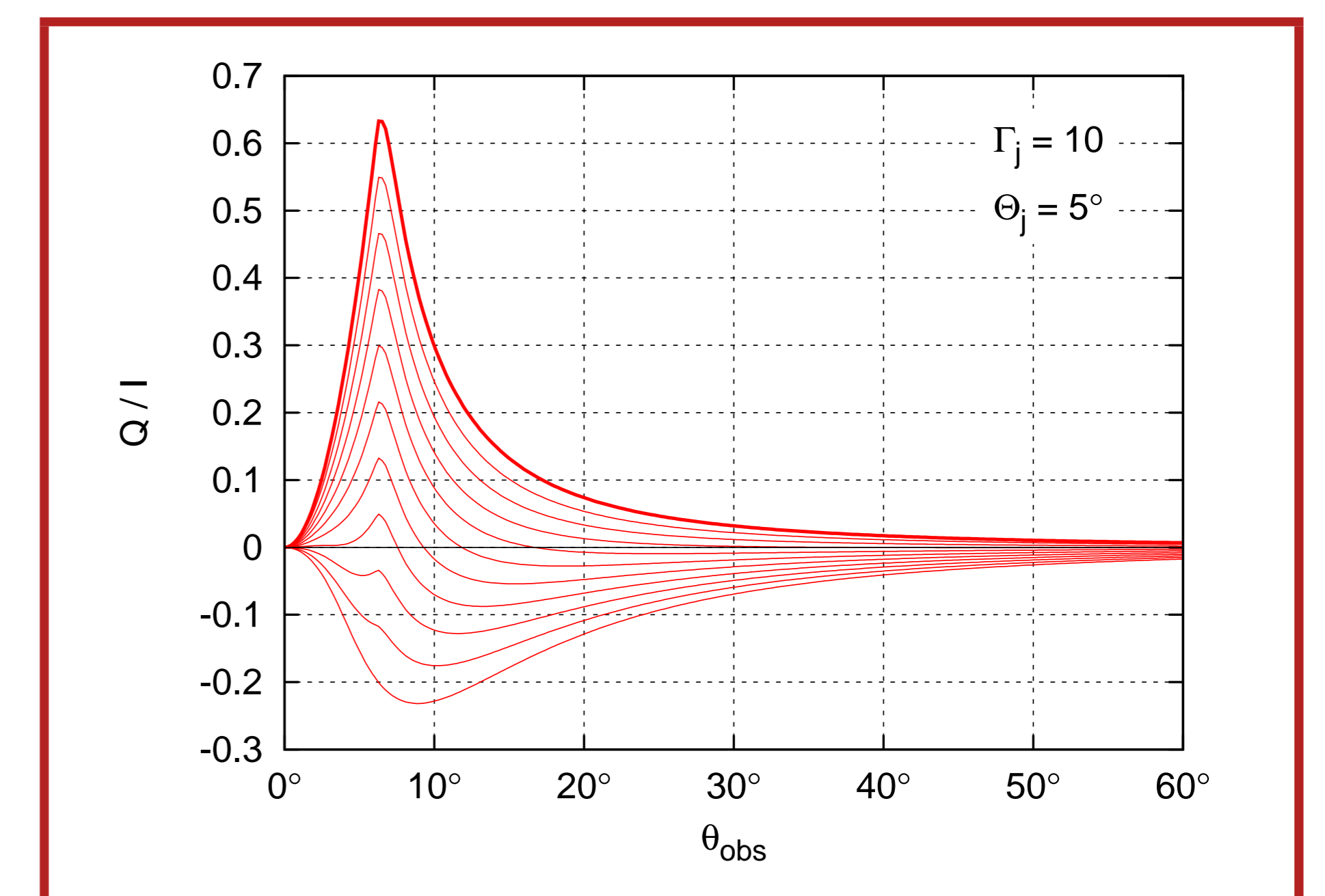


Figure 5: The effect of introducing toroidal magnetic field with energy density being a fraction  $f$  of the total (chaotic+toroidal) magnetic energy density. Plotted are models from  $f = 0$  (pure chaotic MF) to  $f = 1$  (bold line, pure toroidal MF) with steps  $\Delta f = 0.1$ .

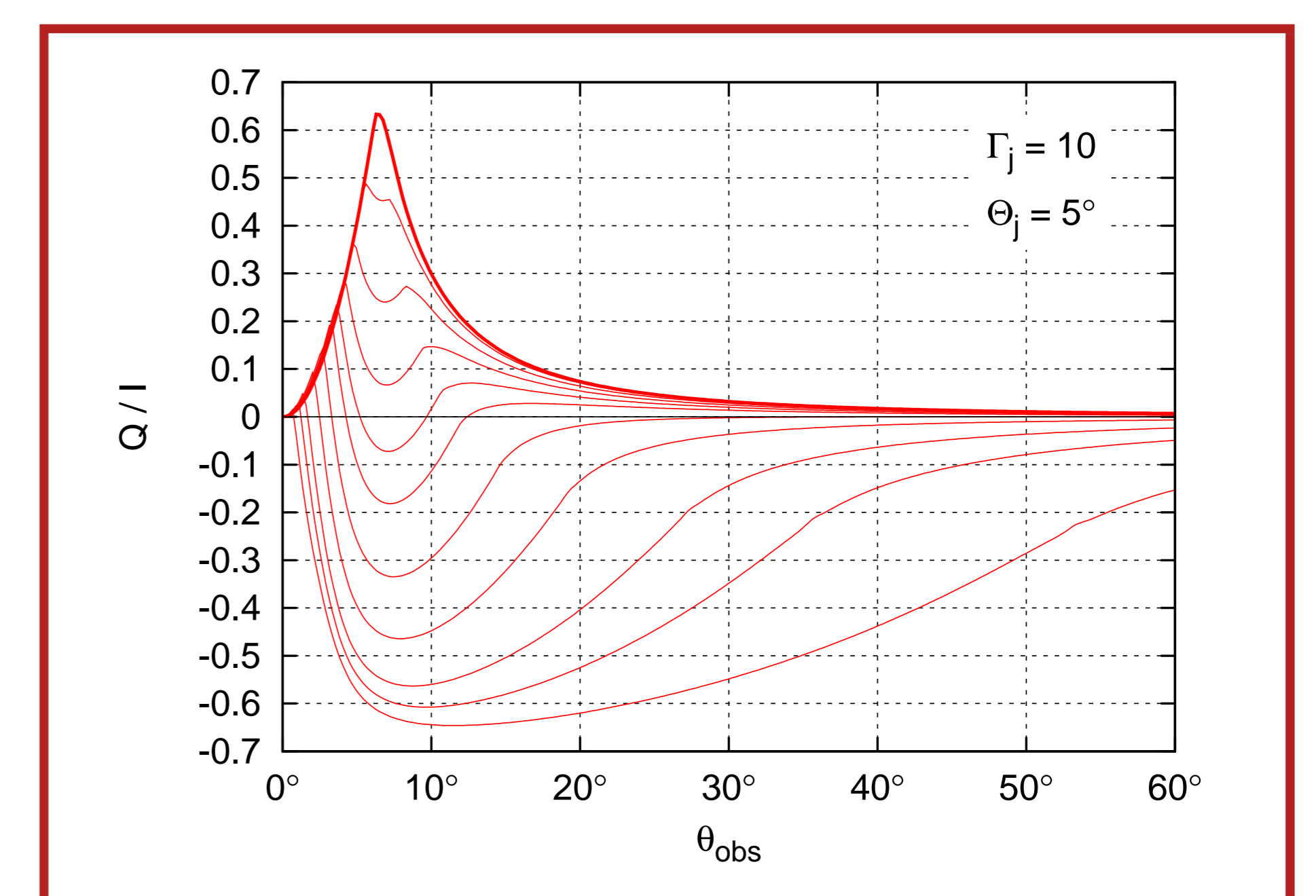


Figure 6: The effect of increasing pitch angle of helical magnetic field. These models are plotted for  $f = 1$  (pure helical MF). Models are calculated for different pitch angle of magnetic field lines at jet maximum width:  $\alpha_B = 0$  (bold line, toroidal MF),  $1^\circ$ ,  $2^\circ$ ,  $3^\circ$ ,  $4^\circ$ ,  $5^\circ$ ,  $7^\circ$ ,  $10^\circ$ ,  $15^\circ$ ,  $20^\circ$  and  $30^\circ$ .

## REFERENCES

- [1] Komissarov, S. S., & Falle, S. A. E. G. 1997, MNRAS, 288, 833
- [2] Stawarz, Ł. et al., 2006, MNRAS, 370, 981
- [3] Sikora, M., Moderski, R., & Madejski, G. M., 2008, ApJ, 675, 71
- [4] Nalewajko, K., & Sikora, M., 2009, MNRAS, 392, 1205
- [5] Lazzati, D., Morsony, B. J., & Begelman, M., 2009, arXiv:0904.2779
- [6] Cawthorne, T. V., Cobb, W. K., 1990, ApJ, 350, 536
- [7] Nalewajko, K., 2009, MNRAS, 395, 524